

# A model for reverse electrowetting with cost-effective materials

Rostislav Rusev<sup>1</sup>, George Angelov<sup>2</sup>, Krasen Angelov<sup>3</sup> and Dimitar Nikolov<sup>4</sup>

<sup>1</sup> Department of Technology and Management of Communication Systems, Faculty of Telecommunications

<sup>2</sup> Department of Microelectronic, Faculty of Electronic Engineering and Technologies

<sup>3</sup> Faculty of Computer Systems and Technologies

<sup>4</sup> Department of Electronics, Faculty of Electronic Engineering and Technologies<sup>4</sup>

Technical University of Sofia

8 Kliment Ohridski Blvd., 1000 Sofia, Bulgaria

{d.nikolov, rusev}@acad.tu-sofia.bg

**Abstract** – This paper, presents a model to predict the energy output from reverse electrowetting energy harvesting system with use of cost-effective materials. Reverse electrowetting on dielectric allows energy to be harvested from spontaneous aperiodic mechanical movements, where conventional energy harvesting approaches are not suitable for due to low energy conversion efficiency and frequency.

**Keywords** – reverse electrowetting-on-dielectric, REWOD, energy harvesting, aperiodic mechanical movements

## I. INTRODUCTION

Transformation of environmental to electrical energy is known as energy harvesting. The notion of energy harvesting dates back centuries ago, especially conversion of the energy from mechanical movement and wind. In recent years, a lot of scientific studies are focused on methods to convert mechanical vibrations and vibration-induced jitter to electrical energy [1]–[4]. However, the developed methods i.e. piezoelectric and electromechanical, have small energy conversion efficiency [5]. This limits the use of mechanical energy harvesting solutions mainly to devices with low consumption. In addition, piezoelectric harvesters are not suitable for vibrations with low frequencies (below 40 Hz) and are tightly coupled to the resonance frequency, which makes them unsuitable for harvesting energy spontaneous aperiodic movements.

Recently, the scientific community drew its attention to an interesting usage of a century old phenomenon i.e. electrowetting (EW) [6]. The traditional use of EW include micro- and nano-fluidics, variable focal length control and electronic displays [7], in contrast the reverse electrowetting-on-dielectric (REWOD) [8] enable design of mechanical energy harvesting system with high conversion efficiency, high power density at low-frequencies of mechanical vibration over a wide range of actuation frequencies. For example in [8] designed and realized energy harvesting devices able to capture mechanical energy with frequency between 0.5 Hz and 350 Hz with energy conversion efficiency up to 75 %. To achieve this, the authors employ a complex set of technological processes to deposit a thin-film hydrophobic layer, with thickness in the range of tens of nanometers, and rare materials.

This paper presents a mathematical model of mechanical energy harvesting system based on reverse electrowetting-on-dielectric constructed with accessible and cost-effective materials. The model will predict the ability of the proposed system to convert mechanical vibrations to electrical energy.

## II. REWOD'S MODEL AND EQUATIONS

The electrowetting phenomenon is defined as “the change in solid-electrolyte contact angle due to an applied potential difference between the solid and the electrolyte” [9]. Consequently, the reverse electrowetting is when external mechanical actuation causes a change in capacitance between electrode and dielectric and the excessive charges flow throughout the load. The concept behind REWOD is shown on Fig. 1, the liquid droplet is placed between electrode and dielectric layer covered with hydrophobic layer. The electrode and dielectric layer are connected to external bias voltage and the load. As the electrode moves the droplet change its area and thus changes the capacitance and if the external bias is held constant excessive charges flow in the load.

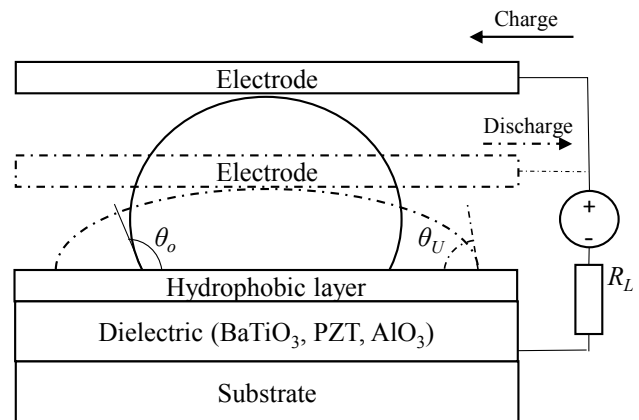


Fig. 1 Electrowetting operation principle

The classical description of contact angle (without external voltage) is defined in Eq. 1

$$\cos \theta_0 = \frac{\gamma_{sa} - \gamma_{sl}}{\gamma_{la}}, \quad (1)$$

where  $\gamma_{sa}$  is the interface tension between solid and air,  $\gamma_{sl}$  is the interface tension between solid and liquid and  $\gamma_{la}$  is the interface tension between liquid and air. The values of interfaces tensions depend on the used materials for liquid, dielectric and surrounding environment (in the presented case - air) and temperature.

The capillary free energy  $E_{cap}$  is given by the Young equation,

$$E_{cap}(\theta) = A_{sa}\gamma_{sa} + A_{sl}\gamma_{sl} + A_{la}\gamma_{la} - V\Delta P, \quad (2)$$

where  $A_{sa}$  is the area of solid/air interface,  $A_{sl}$  is the area solid/liquid interface, and  $A_{la}$  is the area liquid/air interface,  $V$  – liquid droplet volume, and  $\Delta P$  is Laplace pressure. Thus,  $E_{cap}$  depends on  $\Delta P$ , as shown Eq. 1 and 2, given the constant temperature and droplet volume.

Laplace pressure  $\Delta P$  is the differential pressure between the outside and the inside of a curved surface, i.e the outside and the inside of a liquid droplet, and depends on both the surface tension and the geometry of the droplet.  $\Delta P$  is given by the Young-Laplace-Gauss equation,

$$\Delta P = \gamma_{la} \left( \frac{1}{r_1} + \frac{1}{r_2} \right), \quad (3)$$

here  $r_1$  and  $r_2$  are the main radii of curvature of the liquid droplet.

When external voltage is applied, the contact angle is described with Young-Lippmann equation,

$$\cos \theta_{YL}(U) = \cos \theta + \frac{\epsilon_0 \epsilon_d}{2\gamma_{la}d} U^2, \quad (4)$$

where  $\epsilon_d$  is the relative permittivity of the dielectric layer,  $\epsilon_0$  is relative permittivity of vacuum and  $d$  is width of the dielectric layer.

The total energy  $E_{el}(\theta, U)$  is a sum of capillary energy  $E_{cap}(\theta)$  and electrical/electrostatic energy  $E_{el}(\theta, U)$ ,

$$E_{tot}(\theta, U) = E_{cap}(\theta) + E_{el}(\theta, U), \quad (5)$$

Yet, the electrical/electrostatic energy  $E_{el}(\theta, U)$  depends on the total capacitance of the system  $C_{tot}(\theta)$  and the external applied voltage  $U$ , given by,

$$E_{el}(\theta, U) = -\frac{C_{tot}(\theta)U^2}{2}, \quad (6)$$

where the total capacitance  $C_{tot}(\theta)$  is approximately given by,

$$C_{tot} \approx \frac{\epsilon_0 \epsilon_d A_{ld}}{d} \quad (7)$$

If the Laplace pressure is changed, as shown on the Eq. 1-6, then the area liquid-dielectric will be changed and consequently the  $C_{tot}$  will be changed and if the constant external voltage is assumed then the excessive charges will flow throughout the load. Equations 1-6 show the transformation of the mechanical energy to electrical energy through a REWOD phenomenon.

### III. RESULTS AND DISCUSSION

#### A. Model Verification

The Eq. 1-6 are coded in Matlab where  $\Delta P$  is parametrized. Consequently, both the droplet main radii  $r_1$  and  $r_2$  and the capacitance  $C_{tot}$  are calculated in order to predict the energy output the REWOD system.

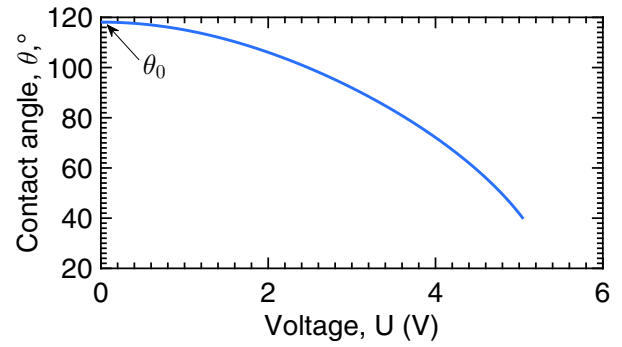


Fig. 2 Contact angle saturation model

The behaviour of the contact angle when external voltage is applied is shown on Fig. 2. The presented model exhibits identical behaviour as theoretical results given in [10]. The parameters of the model are: i) droplet volume – 50  $\mu\text{L}$ , ii) thickness of the dielectric layer – 0.1  $\mu\text{m}$ , iii) permittivity of the dielectric layer – 2.67, iv) permittivity of the liquid – 80, v) dielectric/air surface tension – 12.7 mN/m, vi) liquid/air surface tension – 72.8 mN/m, vi) liquid/dielectric surface tension – 47 mN/m.

Furthermore the verification of the presented model is conducted against the experimental results found in [8]. Both the theoretical model predictions of the presented model and experimental results are shown on Fig. 3. The calculated root-mean-square-error is 10.93 % or 5.04 nJ  $\text{mm}^{-2}$ , which is satisfactory result for the closeness of the proposed model with experimental data.

The standard deviation of the model i.e. root-mean-squared-error is calculated as follows,

$$RMSE, \% \approx \sqrt{\frac{\sum(E_{calc} - E_{exp})^2}{k}} \cdot \frac{100 \cdot k}{\sum E_{exp}}, \quad (8)$$

where  $E_{exp}$  is data from the experiment and  $k = 6$  is the number of experiment data.

Experimental setup in [8] is as follows, a single mercury droplet with area of 1  $\text{mm}^2$  is placed over the Cytop [11], a thin-film fluoropolymer. The Cytop, is deposited on top of tantalum pentoxide ( $\text{Ta}_2\text{O}_5$ ) with thickness tens of nanometers and permittivity of 50. The  $\text{Ta}_2\text{O}_5$  is coated with Cytop a to mitigate surface charge trapping. Mercury has a permittivity of 1.00074 and the capacitance of the plates, where droplet is placed is 16 nF  $\text{cm}^{-2}$ .

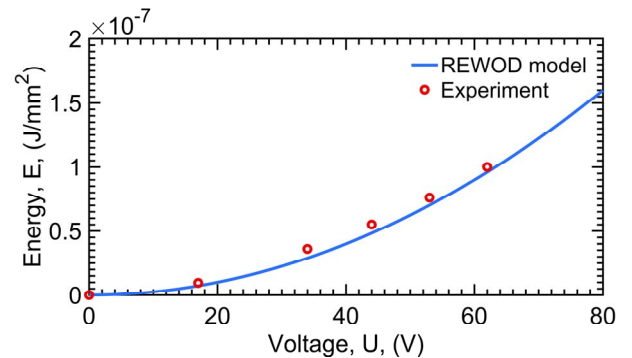


Fig. 3 Electrical energy per cycle per  $\text{mm}^2$ , mercury droplet on cytop dielectric

## B. Barium titanate REWOD model

The presented experimental configuration yields a high-power at a small scale, but to achieve this, one needs a rare materials and precisely controlled technological processes. However, to achieve cost-efficiency and scalability one would trade the energy conversion efficiency and power density for use of abundant materials and processes. In order to achieve that, this paper theoretically study use of two distinct REWOD setups. First setup uses a barium titanate ( $\text{BaTiO}_3$ ) as a dielectric and second lead zirconate titanate ( $\text{Pb}[\text{Zr}_x\text{Ti}_{1-x}]\text{O}_3$ ). For both setups first the energy for one cycle is calculated and for stack of 50 droplets..

The stack consist of  $\text{BaTiO}_3$  covered with thin layer of paraffin [12], droplet of water with NaCl and electrode, the detailed parameters of the stack are shown in Table. 1. As the  $\text{BaTiO}_3$  dielectric constant is highly dependent on the particle size [13], ranging from  $150^1$  to  $5000^2$ , the combined dielectric constant of 254 is used throughout the model.

TABLE 1. BARIUM TITANATE REWOD MODEL

	Material	Property	Value
<b>Dielectric</b>	$\text{BaTiO}_3$	Thickness	1 $\mu\text{m}$
		Permittivity	200
<b>Hydrophilic layer</b>	Paraffin	Thickness	0.2 $\mu\text{m}$
		Permittivity	20
<b>Droplet</b>	Water with NaCl	Volume	5 $\mu\text{L}$
		Permittivity	78.9

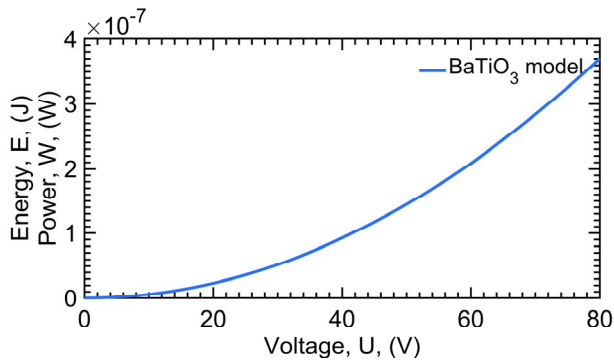


Fig. 4 Energy generated per cycle, power at 1 Hz oscillation

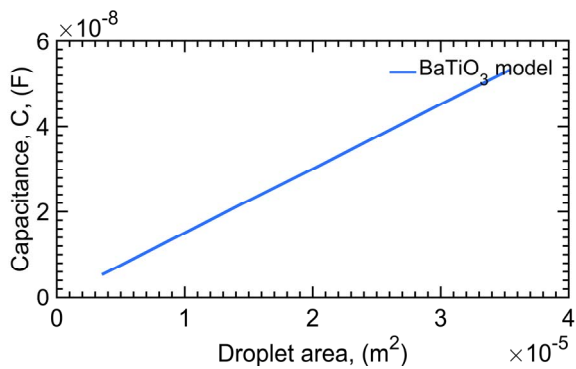


Fig. 5 Capacitance of the REWOD  $\text{BaTiO}_3$  model

Fig. 4 shows the electrical energy generated from single droplet of one cycle or power generated from mechanical actuation with frequency of 1 Hz. The generated electrical energy is highly dependent on the capacitance Eq. 6, and as a result the capacitance is dependent on the droplet area shown in Fig. 5.

The energy generated from one cycle for a voltage at saturation contact angle from the proposed setup with 50 droplets will be 12.23  $\mu\text{J}$ .

## C. Lead zirconium titanate

Table 2 shows the parameters used for REWOD model with lead zirconium titanate,  $\text{Pb}[\text{Zr}_x\text{Ti}_{1-x}]\text{O}_3$ , PZT [14]. The calculations are performed for stack consisting of PZT, droplet of water with NaCl and electrode, the detailed parameters are presented in Table 2. The total dielectric constant, used throughout the calculations, of the stack of PZT and paraffin is 245.

TABLE 2. LEAD ZIRCONIUM TITANATE REWOD MODEL

	Material	Property	Value
<b>Dielectric</b>	PZT	Thickness	1 $\mu\text{m}$
		Permittivity	290
<b>Hydrophilic layer</b>	Paraffin	Thickness	0.2 $\mu\text{m}$
		Permittivity	20
<b>Droplet</b>	Water with NaCl	Volume	5 $\mu\text{L}$
		Permittivity	80

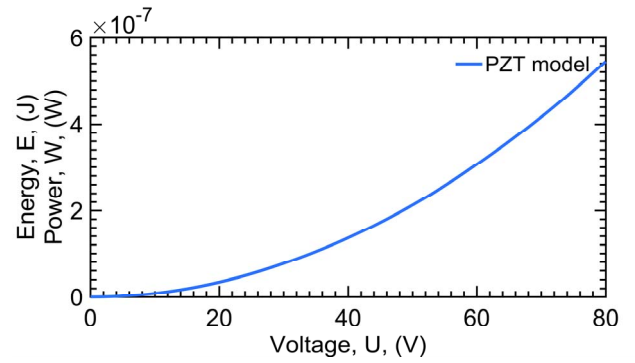


Fig. 6 Energy generated per cycle, power at 1 Hz oscillation

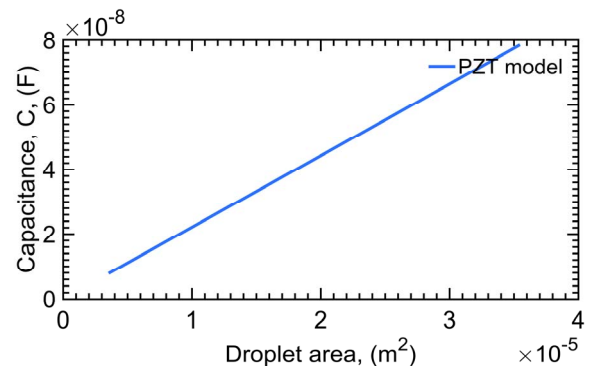


Fig. 7 Capacitance of the REWOD PZT model

<sup>1</sup> When the particle size is  $<100$  nm [15]

<sup>2</sup> When the particle size is  $0.8$   $\mu\text{m}$  [16]

The electrical energy generated per cycle is shown on Fig. 6 and dependence of the stack on droplet area on Fig. 7. The generated energy for the setup of 50 droplets at external voltage at contact saturation angle is 16.62  $\mu\text{J}$ .

#### D. Discussion

The energy generation from REWOD is a straightforward process with intricate balance between material properties, physical dimensions and external circuitry. The electrical energy density is highly dependent on the capacitance between electrode and dielectric, as shown on the Eq. 6. The capacitance itself is proportionally dependent on the droplet area and inversely proportional to the thickness of dielectric layer. Increase of the dielectric thickness will decrease the generated energy due to the decrease in total capacitance Eq. 7.

Another aspect of capacitance is permittivity of the dielectric, the higher the permittivity, the higher capacitance. However, increasing solely the permittivity of dielectric will decrease contact angle saturation and area of the droplet. In order to achieve higher energy density, the higher capacitance is needed, so higher droplet area and thinner dielectric layer with careful consideration of the permittivity of the dielectric.

Frequency behaviour and losses in scaling of the REWOD system with more droplets in parallel is another subject. Both will increase the energy output and make it useful for post-processing and storing. However, the presented model does not explicitly include the frequency behaviour, due to the fact that additional loss mechanisms are at play. The presented model allows only some rough calculations when taking into account frequency and scaling.

## IV. CONCLUSION

The model presented in this paper, describes the behaviour of the energy generation from reverse electrowetting phenomenon. REWOD allows energy to be harvested from spontaneous aperiodic mechanical movements, which conventional energy harvesting approaches i.e. piezoelectric and electromechanical. REWOD is easily scalable, which in turns will increase energy output.

The presented BaTiO<sub>3</sub> and PZT setups with 50 droplets prove to harvest 12.23  $\mu\text{J}$  and 16.62  $\mu\text{J}$  respectively. When this is scaled with higher frequency and optimized geometrical shapes it would be enough to be powered with human locomotion and spontaneous aperiodic mechanical actuations.

## V. ACKNOWLEDGEMENT

This paper is based on work supported by Research and Development Sector of Technical University Sofia, Contract № 171IPP0014-03/date 03.2017.

#### REFERENCES

- [1] J. Shen, C. Wang, P. C. Luk, D.-M. Miao, D. Shi, and C. Xu, "A Shoe-Equipped Linear Generator for Energy Harvesting," *IEEE Trans. Ind. Appl.*, vol. 49, no. 2, pp. 990–996, Mar. 2013.
- [2] N. S. Shenck and J. A. Paradiso, "Energy scavenging with shoe-mounted piezoelectrics," *IEEE micro*, vol. 21, no. 3, pp. 30–42, 2001.
- [3] D. Han and V. Kaajakari, "Microstructured polymer for shoe power generation," *TRANSDUCERS 2009 - 2009 Int. Solid-State Sensors, Actuators Microsystems Conf.*, pp. 1393–1396, Jun. 2009.
- [4] H. Yang, S. Hong, B. Koo, D. Lee, and Y. Kim, "High-performance reverse electrowetting energy harvesting using atomic-layer-deposited dielectric," *Nano Energy*, vol. 31, no. September 2016, pp. 450–455, 2016.
- [5] G. Poulin, E. Sarraute, and F. Costa, "Generation of electrical energy for portable devices: Comparative study of an electromagnetic and a piezoelectric system," *Sensors Actuators, A Phys.*, vol. 116, no. 3, pp. 461–471, Oct. 2004.
- [6] F. Mugele, M. Duits, and D. van den Ende, "Electrowetting: A versatile tool for drop manipulation, generation, and characterization," *Adv. Colloid Interface Sci.*, vol. 161, no. 1–2, pp. 115–123, Dec. 2010.
- [7] Y.-P. Zhao and Y. Wang, "Fundamentals and applications of electrowetting," *Rev. Adhes. Adhes.*, vol. 1, no. 1, pp. 114–174, 2013.
- [8] T. Krupenkin and J. A. Taylor, "Reverse electrowetting as a new approach to high-power energy harvesting," *Nat. Commun.*, vol. 2, no. 448, pp. 1–7, 2011.
- [9] Y. Xu, D. Xu, and J. Liang, *Biological and Medical Physics, Biomedical Engineering Biological and Medical Physics*. 2007.
- [10] D. Klarman and D. Andelman, "A model of electrowetting, reversed electrowetting, and contact angle saturation," *Langmuir*, vol. 27, no. 10, pp. 6031–6041, 2011.
- [11] "Cytos technical information," 2013. [Online]. Available: <http://www.agcce.com/cytop-technical-information/>. [Accessed: 10-Jun-2017].
- [12] Encyclopaedia Britannica, "Dielectric constant." [Online]. Available: <https://www.britannica.com/science/dielectric-constant#ref216281>. [Accessed: 09-Jul-2017].
- [13] L. Wu *et al.*, "Dielectric properties of barium titanate ceramics with different materials powder size," *Ceram. Int.*, vol. 35, no. 3, pp. 957–960, Apr. 2009.
- [14] M. D. Aggarwal, A. K. Batra, P. Guggilla, and M. E. Edwards, "Pyroelectric Materials for Uncooled Infrared Detectors: Processing, Properties, and Applications," *Natl. Aeronaut. Sp. Adm.*, no. March, 2010.
- [15] "Barium titanate(IV) nanopowder (cubic crystalline phase)," *SIGMA ALDRICH*. [Online]. Available: <http://www.sigmaaldrich.com/catalog/product/aldrich/467634?lang=en&region=BG>. [Accessed: 14-Jun-2017].
- [16] B. W. Lee and K. H. Auh, "Effect of grain size and mechanical processing on the dielectric properties of BaTiO<sub>3</sub>," *J. Mater. Res.*, vol. 10, no. 6, pp. 1418–1423, Jun. 1995.